atoms such as oxygen or nitrogen is generally thought to be faster than proton transfer to carbon centers, owing to the availability of a localized electron pair in the former case.[47] Our study raises the possibility that proton transfer to carbon centers may also be quite fast in some cases. An important question for our future study is whether stabilization of radical cations at low temperature is also possible in neat alcohols, ethers, etc., allowing their study by FDMR.

The importance of ion-molecule reactions in the overall chemistry induced by ionizing radiation in hydrocarbons remains to be seen. The fact that the detection sensitivity of the FDMR technique depends on the lifetime of the radical ion species introduces a bias toward longer lived ion pairs. In the FDMR experiment electron scavenging by the scintillator gives rise to less mobile scintillator anions, extending the time available for the partner alkane radical cations to react. This is at once an advantage and a disadvantage of the technique. Delaying recombination amplifies the differences in reactivity of radical cations of different alkanes. But the fact that FDMR only probes a small fraction of events occurring relatively late in time makes it difficult to obtain quantitative estimates of the relative yields of various reaction pathways.

4. Conclusions

In this paper we have discussed various optically detected EPR observations of alkane radical cations in liquid and solid hydrocarbons. We conclude that *ion-molecule reactions* such as proton transfer or H-atom transfer account for the transient nature of alkane radical cations in hydrocarbons. The details of the ion-molecule reactions of alkane radical cations are yet to be fully delineated since factors in addition to molecular shape and spin density in the radical cation must be considered.

Acknowledgment. J. Gregar provided us with the Suprasil FDMR and EPR sample cells. We thank R. H. Lowers for his skillful operation of the Van de Graaff and other technical support and acknowledge him upon his retirement for his many years of valued service and friendship. We acknowledge helpful discussions with X.-Z. Qin, M. C. Sauer, Jr., and C. D. Jonah.

Registry No. 2,2,3,3-Tetramethylbutane radical cation, 68842-40-0; bicyclopentyl radical cation, 75840-32-3; *cis*-bicyclo[4.3.0]nonane radical cation, 123807-66-9; tricyclo[5.2.1.$0^{2,6}$]decane radical cation, 123807-67-0; methylcyclohexane radical cation, 82166-21-0; *cis*-1,4-dimethylcyclohexane radical cation, 123807-68-1; *trans*-1,2-dimethylcyclohexane radical cation, 121054-99-7; perhydrofluorene radical cation, 123807-69-2; adamantane radical cation, 123726-15-8; bicyclo[3.3.0]octane radical cation, 123807-70-5.

(44) Shiotani, M.; Nagata, Y.; Tasaki, M.; Sohma, J.; Shida, T. *J. Phys. Chem.* **1983**, *87*, 1170.
(45) Kubodera, H.; Shida, T.; Shimokoshi, K. *J. Phys. Chem.* **1981**, *85*, 2583.
(46) Lewis, F. *Acc. Chem. Res.* **1986**, *19*, 401.
(47) Kresge, A. J. *Acc. Chem. Res.* **1975**, *8*, 354.

Adsorption and Reactions of Cyclic Sulfides on Mo(110)

Maria José Calhorda,[†,‡] Roald Hoffmann,*[,‡] and Cynthia M. Friend[§]

Contribution from the Department of Chemistry and Materials Science Center, Cornell University, Ithaca, New York 14853-1301, and Department of Chemistry, Harvard University, Cambridge, Massachusetts 02138. *Received December 12, 1988*

Abstract: Molecular orbital calculations of the chemisorption and reactivity of ethylene sulfide and trimethylene sulfide on Mo(110) are presented and compared to similar binding in model-discrete Mo complexes. Our calculations suggest preferred bonding of the cyclic sulfides on 2- or 3-fold sites of the surface, by the expected S-lone pair donor mechanism. The concerted elimination of ethylene or cyclopropane is much easier on the surface than it is in model organometallic molecules. The activation barrier for ethylene sulfide decomposition calculated is substantially smaller than that for trimethylene sulfide. Various nonconcerted mechanisms and the role of coadsorbed sulfur and hydrogen are also probed.

Hydrodesulfurization is a widely used process by which fuel feedstocks react with a molybdenum sulfide catalyst to afford hydrocarbons with lower sulfur content. Several kinds of sulfur derivatives, both aromatic and aliphatic, are found in the raw materials, and considerable effort has been dedicated toward understanding how the reactions occur.[1] Often, simpler models than the actual catalyst are used for that, namely single-crystal transition-metal surfaces.[2]

The molybdenum(110) face has been chosen, due to its stability toward reconstruction, by Friend and co-workers to study systematically the reactions of cyclic sulfides[3] and linear thiols.[4] With the help of several complementary experimental techniques such as temperature-programmed desorption, X-ray photoelectron, and high-resolution electron energy loss spectroscopy, they have been able to establish three distinct reactivity patterns. These three pathways are indicated in **1**, depicting how trimethylene sulfide reacts after adsorption onto the Mo(110) face.

Pathway A leads to cyclopropane formation by intramolecular elimination. An intermediate adsorbed thiolate species is formed in B. The same intermediate is detected directly when a different precursor, propanethiol, reacts with the surface.

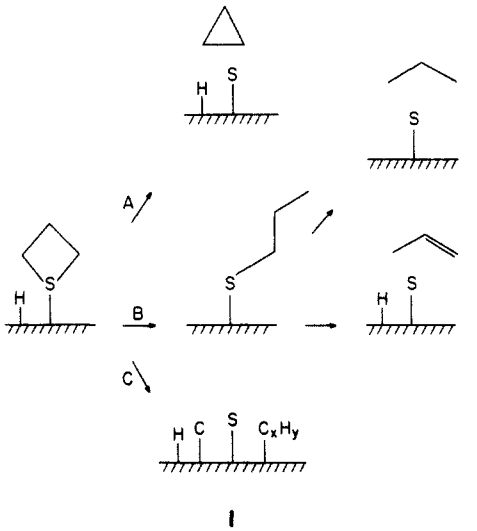

1

[†] Permanent address: Centro de Quimica Estrutural, Instituto Superior Técnico, 1096 Lisbon Codex, Portugal.
[‡] Cornell University.
[§] Harvard University.

0002-7863/90/1512-50$02.50/0

The adsorbed thiolate species can react further breaking the C–S bond, either by forming another C–H bond or losing another H to the surface, yielding respectively alkanes or alkenes. Complete decomposition occurs in pathway C, resulting in surface sulfur, carbon, and hydrocarbon fragments.

This kind of reactivity appears to be quite general for adsorbed thiolates: for instance, following the same trends, phenylthiolate adsorption results in gaseous benzene and surface benzyne. However, cyclic sulfides, depending on ring size, react differently on Mo(110). Pathway B is not observed for ethylene sulfide, whereas intramolecular elimination (A) does not occur for ring sizes greater than four.

We would like to understand how the different sulfur-containing species interact with the molybdenum surface and what electronic factors govern their reactivity. Let us note that these reactions occur in the presence of hydrogen, which is both an impurity impossible to eliminate and a product from S–H bond cleavage in the case of thiol reactions. Also, as reactions proceed, more and more surface carbon and sulfur are formed, changing the reactive capabilities of the surface.[3f]

Gaining some knowledge about the reactivity of sulfur-containing species on a molybdenum(110) surface may help us to understand how real catalytic hydrodesulfurization takes place under more complicated experimental conditions. Many of the studies done concern thiophene, which is considered one of the most difficult molecules to desulfurize.[2,5] Molecular thiophene complexes have been synthesized and used as models for hydrodesulfurization behavior, with variable success.[6]

Some discrete molecular complexes are available, and we shall use them as models for coordination sites and geometries. Also, understanding how a cyclic sulfide or thiolate interacts with a mono- or binuclear molybdenum complex will help us to interpret its interaction with a two-dimensional surface. These two approaches, molecular and extended surface, are conceptually different, but should be complementary in their results.

The calculations done are of the extended Hückel type,[7] and the tight-binding method[8] was used to study the two-dimensional infinite surface. Details are given in the text and in the Appendix.

The Adsorbates

In the following study, we shall consider two adsorbates, SC_2H_4 (ethylene sulfide) and SC_3H_6 (trimethylene sulfide) as models for the different reactivity patterns of cyclic sulfides on Mo(110).

So far nothing is known about the geometry of these heterocycles after adsorption on the surface. One discrete molecular complex of ethylene sulfide has been characterized by Rauchfuss and co-workers.[9] It is a $CpRu(PPh_3)_2(SC_2H_4)^+$ molecule, and the geometry of the ethylene sulfide ring in it is similar to that of the free molecule. In our calculations we take the experimentally observed free molecule structures, from microwave spectroscopy for ethylene sulfide[10a] and from gas electron diffraction for trimethylene sulfide.[10b]

Ethylene sulfide is a planar molecule with S–C bonds 1.815 Å long and a C–C bond of 1.484 Å. Its frontier molecular orbitals are shown in **2**. The LUMO, $2b_1$, both S–C and C–C antibonding, is quite high in energy. The HOMO, $1b_2$, and SHOMO, $2a_1$, are respectively the π and σ sulfur lone pairs, while the next orbital, $1b_1$, is strongly S–C bonding but C–C antibonding. Depopulation of this orbital may be important in weakening the S–C bond and simultaneously strengthening the C–C bond. This would put the system on the way to produce gaseous ethylene and surface sulfur.

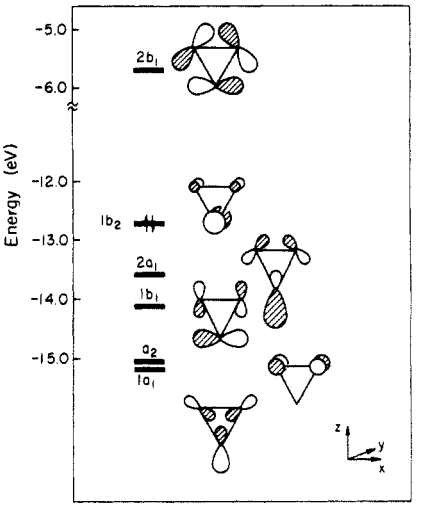

2

Trimethylene sulfide was experimentally found to be nonplanar. The folding angle between the C–C–C and C–S–C planes is 26°, and the S–C and C–C bond lengths are respectively 1.85 and 1.549 Å. The two sulfur-bonded carbon atoms are 2.294 Å apart. The planar four-membered ring is about 0.6 eV higher in energy, according to our calculations.

The frontier molecular orbitals for folded trimethylene sulfide are given in **3**. The LUMO lies at a higher energy than for ethylene sulfide and the two highest occupied MOs are again the π and σ sulfur lone pairs.

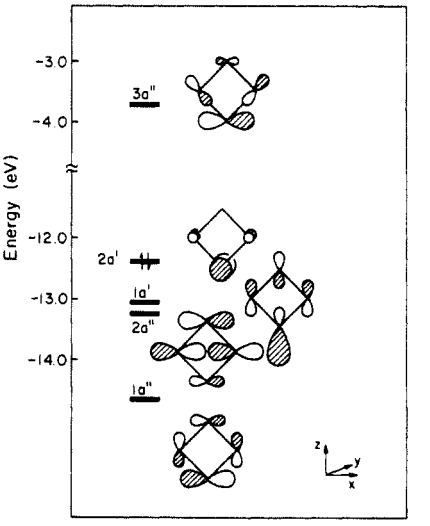

3

(1) (a) Somorjai, G. A. "The Building of Catalysts: A Molecular Surface Science Approach"; Wei, J. "Toward the Design of Hydrodemetallation Catalysts" In *Catalyst Design—Progress and Perspectives*; Hegedus, L. L., Ed.; John Wiley & Sons: New York, 1987. (b) Chianelli, R. R. *Catal. Rev.-Sci. Eng.* **1984**, *26*, 361. (c) Bartholomew, C. H.; Agrawal, P. K.; Katzer, J. R. *Adv. Catal.* **1982**, *31*, 135.

(2) Long, J. F.; Masel, R. I. *Surf. Sci.* **1987**, *183*, 44.

(3) (a) Friend, C. M.; Roberts, J. T. *Acc. Chem. Res.* **1988**, *21*, 394. (b) Friend, C. M.; Roberts, J. T. *J. Am. Chem. Soc.* **1987**, *109*, 7899. (c) Friend, C. M.; Roberts, J. T. *J. Am. Chem. Soc.* **1987**, *109*, 3872. (d) Friend, C. M.; Roberts, J. T. *J. Am. Chem. Soc.* **1986**, *108*, 7204. (e) Friend, C. M.; Roberts, J. T. *J. Am. Chem. Soc.* In preparation. (f) Friend, C. M.; Roberts, J. T. *Surf. Sci.* **1988**, *202*, 405.

(4) (a) Roberts, J. T.; Friend, C. M. *J. Chem. Phys.* **1988**, *88*, 7172. (b) Roberts, J. T.; Friend, C. M. *J. Phys. Chem.* **1988**, *92*, 5205. (c) Roberts, J. F.; Friend, C. M. *Surf. Sci.* **1987**, *198*, L321; *J. Am. Chem. Soc.* **1988**, *110*, 4423.

(5) (a) Roberts, J. T.; Friend, C. M. *Surf. Sci.* **1987**, *186*, 201. (b) Zonnevylle, M. C.; Hoffmann, R.; Harris, S. *Surf. Sci.* **1988**, *199*, 320. (c) Kelly, D. G.; Odriozola, Y. A.; Somorjai, G. A. *J. Phys. Chem.* **1987**, *91*, 5695.

(6) (a) Huckett, S. C.; Miller, L. L.; Jacobson, R. A.; Angelici, R. J. *Organometallics* **1988**, *7*, 686. (b) Ogilvy, A. E.; Draganjac, M.; Rauchfuss, T. B.; Wilson, S. R. *Organometallics* **1988**, *7*, 1171. (c) Chaudret, B.; Jalon, F. A. *J. Chem. Soc., Chem. Commun.* **1988**, 711.

(7) (a) Hoffmann, R. *J. Chem. Phys.* **1963**, *39*, 1397. (b) Hoffmann, R.; Lipscomb, W. N. *J. Chem. Phys.* **1962**, *36*, 2179, 3489; **1962**, *37*, 2872.

(8) (a) Whangbo, M.-H.; Hoffmann, R. *J. Am. Chem. Soc.* **1978**, *100*, 6093. (b) Whangbo, M.-H.; Hoffmann, R.; Woodward, R. B. *Proc. R. Soc. Chem.* **1979**, *A366*, 23.

(9) Amarasekera, J.; Rauchfuss, T. B.; Wilson, S. R. *J. Am. Chem. Soc.* **1988**, *110*, 2332.

(10) (a) Okiye, K.; Hirose, C. *Chem. Phys. Lett.* **1974**, *24*, 111. (b) Karakida, K.; Kuchitsu, K. *Bull. Chem. Soc. Jpn.* **1975**, *48*, 1691.

These molecules will bond to a metal atom essentially through the sulfur lone pairs, but lower molecular orbitals may be involved in some situations as, for instance, when they are bridging two metal atoms. Let us consider ethylene sulfide and two limiting coordination geometries, shown in **4**.

4

The total energy changes while going from the perpendicular coordination (**4**, left) to the parallel one (**4**, right). This is shown in **5**, for ML_n = $Mo(CO)_5$, MoH_4^{4-}, and CH_3^+.

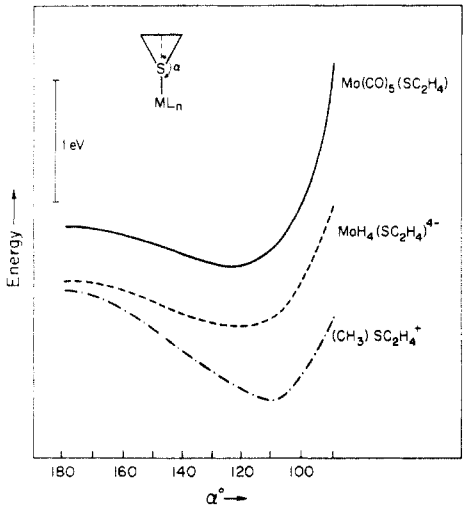

5

In general sulfonium salts are strongly pyramidal, and our calculations reproduce this fact. Steric constraints play a role, as the ethylene sulfide hydrogens approach other atoms. This is why the small CH_3 group gives the largest bending angle. In the one known organometallic complex of ethylene sulfide, α is 112°.[9]

The way SC_2H_4 binds to a square-planar MoH_4^{4-} (d^6,Mo(0), in anticipation of the Mo surface) is analyzed in the interaction diagram of Figure 1 for the perpendicular, higher symmetry, geometry. On the right side are the orbitals of SC_2H_4, as shown before in **2**. The orbitals on the left are those of a square-planar complex, with the typical four below one splitting of the d levels.[11] The highest one is not seen in this energy window.

Large overlaps are present between the sulfur σ lone pair ($2a_1$ and $1a_1$) and empty $3a_1$ (z^2) and $4a_1$ (z) of the metallic fragment. Back-donation from $2b_1$ (xz) to the ethylene sulfide LUMO is negligible. The sulfur ligand acts as a σ donor. The ligand HOMO, $1b_2$, is involved in a weak four-electron destabilizing interaction with $2b_2$ (yz), the antibonding molecular orbital being the HOMO of the complex.

When the three-membered ring bends, the symmetry is lowered and the HOMO can interact with $3a_1$ and $4a_1$ of MoH_4^{4-}. There is a better energy matching between these orbitals and a stronger interaction results. The previous destabilizing interaction is relieved, as the overlap population between ligand HOMO and $2b_2$ of the MoH_4^{4-} fragment drops from −0.032 to −0.008, making the HOMO of the complex almost nonbonding. A better bond is formed, as shown by the minimum in the total energy curve (**5**) for large bending angles.

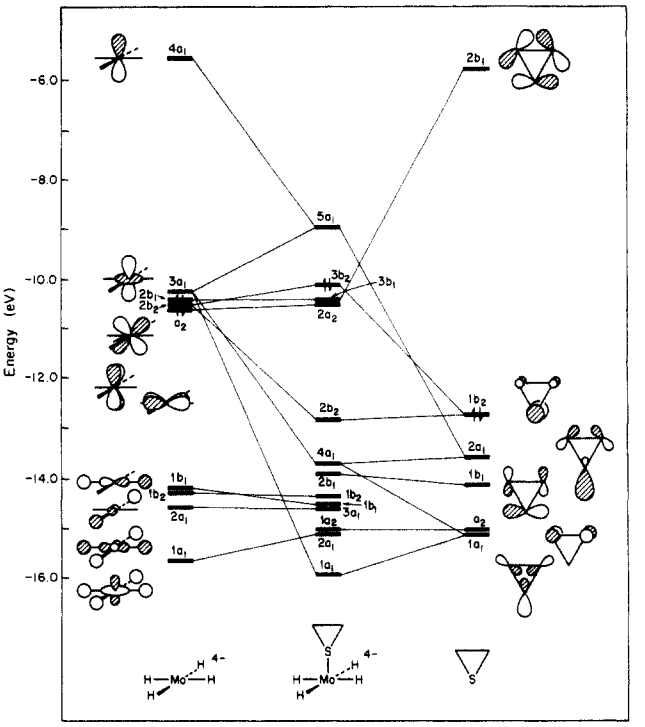

Figure 1. Interaction diagram for the model complex $MoH_4(SC_2H_4)^{4-}$.

Let us now consider ethylene sulfide acting as a bridging ligand. There are two extreme geometries—parallel, **6**, and perpendicular, **7**. Furthermore one could imagine bending starting from either conformation.

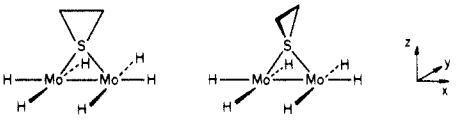

6 **7**

Although in the parallel form some stabilization (0.3 eV) is achieved by bending, the initial perpendicular geometry is still 1.3 eV more stable. In comparing the perpendicular and parallel geometries, the σ interaction between the $2a_1$ lone pair and symmetric combinations of Mo z^2 and xz orbitals will be similar. However, for the perpendicular geometry a strong interaction develops, **8**, between the antisymmetric combinations of z^2 and xz and the HOMO.

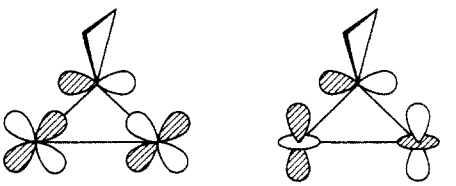

8

An analogous interaction for the parallel geometry would involve $1b_1$, which is not such a good donor and has a smaller localization on the sulfur. It would be weaker due both to energy and overlap reasons. The resulting species would then be less stable.

An example of a bridging cyclic sulfide (tetrahydrothiophene) adopting a perpendicular geometry is seen in the complex $[Nb_2Cl_6(\mu\text{-tetrahydrothiophene})_3]^{2-}$ (**9**).[12]

(11) Albright, T. A.; Burdett, J. K.; Whangbo, M.-H. *Orbital Interactions in Chemistry*; Wiley Interscience: New York, 1985.

(12) Cotton, F. A.; Diebold, M. P.; Roth, W. J. *J. Am. Chem. Soc.* **1987**, *109*, 5506.

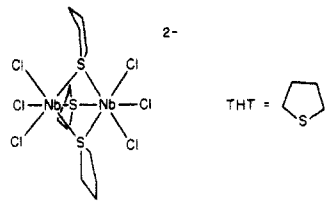

9

Our calculations, not reported here in detail, show that the bonding preferences of trimethylene sulfide (SC_3H_6) are similar to those of ethylene sulfide.

The molecular complexes used as models are related to the molybdenum environment in the surface as in both the molybdenum atoms have four nearest neighbors in the same plane. The symmetry is higher in these discrete molecules, making the analysis simpler, but the results are qualitatively the same compared to more realistic models, for instance, considering the molybdenum atom with six nearest neighbors, as in the (110) face of the BCC structure, four in the same plane and two below it.

The Reactivity of the Adsorbates

Let us imagine a concerted mechanism that leads from an ethylene sulfide complex to a sulfide, with formation of free ethylene, **10**, in a process similar to that proposed on the Mo(110) surface.

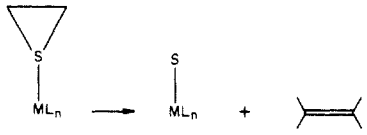

10

Similarly, we shall have **11** for trimethylene sulfide, leading to cyclopropane.

11

The related reaction between ethylene oxide and the tungsten complex $WCl_2(PMePh_2)_4$ has been studied theoretically.[13] However, this reaction differs from the one we want to study in that, after breaking the C–O bonds, both the oxygen and the ethylene remain bound to the metal center. In the surface reaction of ethylene sulfide, ethylene is directly evolved into the gas phase with 85% selectivity at the adsorption temperature of 120 K and none remains bound directly to the surface. Furthermore, ethylene itself adsorbs and irreversibly decomposes on clean and sulfur-covered Mo(110) with high probability under the same conditions. These kinetic data show that gaseous product does not proceed through a surface-bound ethylene intermediate and are suggestive of a concerted transition state where the ethylene product is formed with a large component of momentum perpendicular to the surface.

Let us then *assume* a concerted reaction: the two S–C bonds stretch simultaneously, while the hydrogens relax toward a planar ethylene geometry by the end of the reaction, as indicated in **12**. The C–C bond length was kept constant.

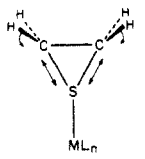

12

(13) Schiøtt, B.; Jørgensen, K. A. Private communication.

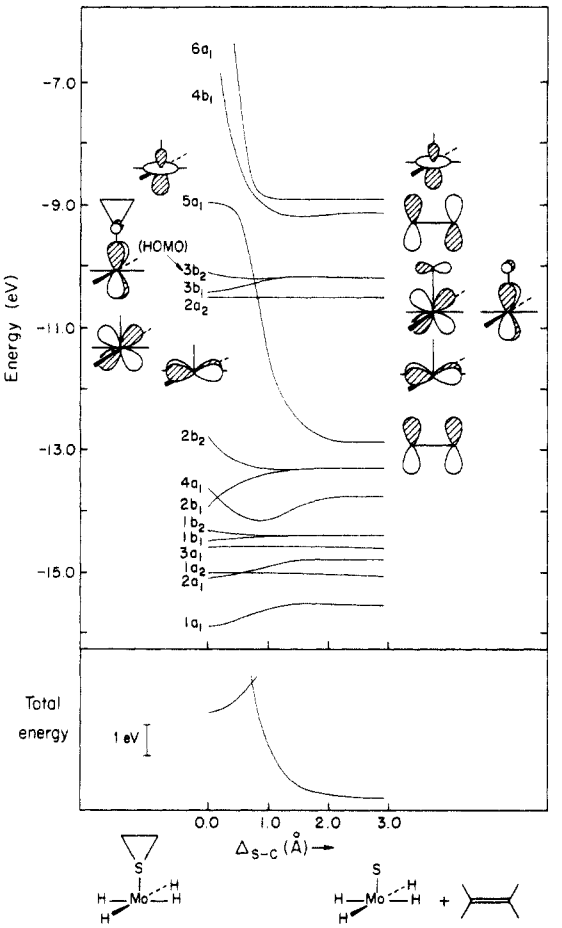

Figure 2. Walsh diagram and total energy change for the reaction $MoH_4(SC_2H_4)^{4-} \rightarrow MoH_4S^{4-} + C_2H_4$, as a function of the stretching of the S–C bond.

Contracting it from 1.484 to 1.34 Å (in free ethylene) will lead to further stabilization. The change of total energy and the Walsh diagram along this hypothetical reaction path are shown in Figure 2, as a function of the S–C bond stretching.

C_{2v} symmetry is retained throughout the reaction. There are several avoided crossings. One originates from a high-energy S–C antibonding orbital that cannot correlate with the π orbital of the forming ethylene, which is much more stable. Initially, there are six electrons in the three lowest d orbitals. By the end of the reaction, π will be occupied and only four electrons remain in the metal d orbitals. There is a formal oxidation state change from Mo(0) to Mo(II), as the sulfide complex is formed. The reaction is forbidden for this electron count, with a computed activation energy close to 1 eV.

Let us compare these results to those obtained when the reacting ethylene sulfide is bridging two molybdenum atoms, in the model compound $Mo_2H_6(SC_2H_4)^{6-}$ (perpendicular geometry), **7**.

The metal fragment is derived from two square-planar units and eight d orbitals are now present, the other two having too high energies. The symmetry is still C_{2v} and the assumed reaction pathway is exactly the same as before. The Walsh diagram and the change in total energy are shown in Figure 3. Generally, the energy varies in the same way as was observed in the previous model and analogous level crossings are observed here between orbitals of a_1 symmetry.

The same essentially holds if we take other models that more closely resemble the type of molybdenum coordination on the (110) face, with six nearest neighbors, four in the surface plane (but not arranged in a square) and two below.

What happens if we now look at the reaction represented in **11**, that is, formation of cyclopropane and a sulfide complex from the trimethylene sulfide complex? The model is $MoH_4(SC_3H_6)^{4-}$, and the trimethylene sulfide ligand is bound as shown in the right side of **4**, with a M–SCC plane angle of 130°.

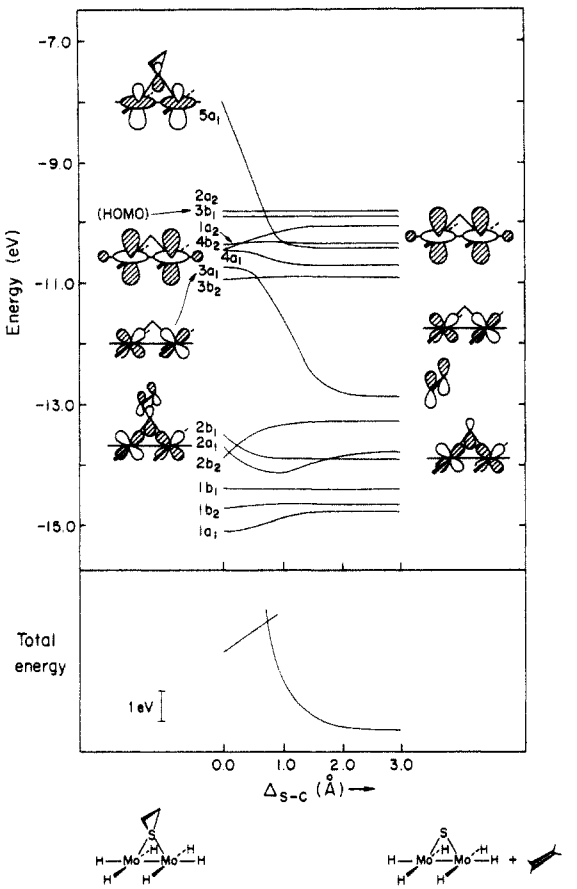

Figure 3. Walsh diagram and total energy change for the reaction $Mo_2H_6(SC_2H_4)^{6-} \rightarrow Mo_2H_6S^{6-} + C_2H_4$, as a function of the stretching of the S–C bond.

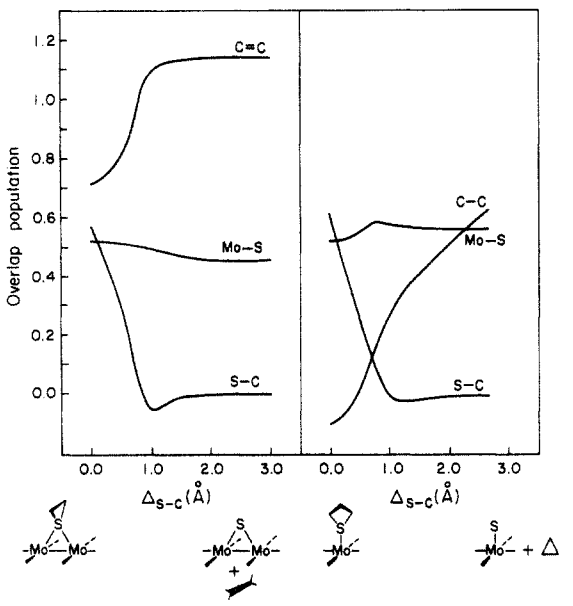

Figure 4. Evolution of the S–C, C–C, and Mo–S overlap populations along the pathways described in the text for the reactions $Mo_2H_6(SC_2H_4)^{6-} \rightarrow Mo_2H_6S^{6-} + C_2H_4$ (left) and $MoH_4(SC_3H_6)^{4-} \rightarrow MoH_4S^{6-} + C_3H_6$ (right).

We must start by defining a reaction path. Here there are more severe geometrical changes to contend with. While for ethylene sulfide a single carbon–carbon bond became a double bond, now a new carbon–carbon bond has to be formed starting from atoms that are relatively far apart. In **13** are shown the geometrical parameters to be varied: the S–C bond is stretched; the two carbon atoms approach each other to form a bond; the hydrogens bound to them reorient.

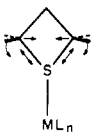

13

In the end the three C–C bonds in the cyclopropane product have the same length (but, as for ethylene, we did not allow for relaxation to the true C–C bond length which is 1.515 Å, compared to 1.549 Å in SC_3H_6—the difference is small). The symmetry is now lower than for the formation of ethylene. Due to the folding of the SC_3H_6 ring, only one mirror plane is left to the molecule, instead of two.

The Walsh diagram is very similar to the one in Figure 2. Instead of a π orbital, a stabilized level corresponding to the newly formed C–C bond is observed at low energies toward the end of the reaction. It derives from a high-energy antibonding orbital, but avoided crossings occur with metal d orbitals of the same symmetry. The shape of the total energy curve, **14**, is similar to the ones seen before. The reaction is still forbidden, with a relatively small activation energy.

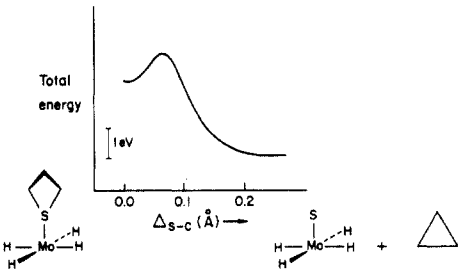

14

Let us now look at the evolution of the S–C, Mo–S, and C–C overlap populations along the reaction pathway, as they give us an indication of how bonds are being formed or broken.

They are represented in Figure 4 for the two reacting species: ethylene sulfide in $Mo_2H_6(SC_2H_6)^{6-}$ and trimethylene sulfide in $MoH_4(SC_3H_6)^{4-}$. There are no great changes in the Mo–S bond while the S–C bond is broken and the C–C is strengthened (for SC_2H_4) or formed (SC_3H_6). The changes are relatively smooth, some discontinuities arising from the above-mentioned avoided crossings. The proposed pathway seems reasonable.

We are now ready to proceed to the study of the surface reactions.

The Mo(110) Surface

Molybdenum has a body centered cubic structure with $a = 3.15$ Å.[14] The 110 face is centered rectangular, but we use a $P(2\times2)$ unit cell, **15**.

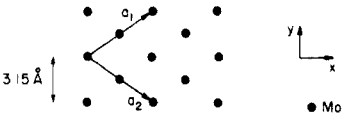

15

The atoms in the second layer occupy positions in the center of the rhombus, **16**, and the stacking is ABAB..., that is the third layer is exactly below the first one.

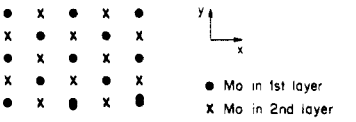

16

(14) Ashcroft, N. W.; Mermin, N. D. *Solid State Physics*; Saunders College: Philadelphia, 1976.

Table I. Binding Energies and Overlap Populations for Ethylene Sulfide on Mo(110)

	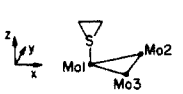					
adsorption site, geometry	**18a**, perp.	**18a**, bent 45°	**18d**, perp.	**18e**, perp.	**18f**, perp.	**18f**, bent 50°
B.E.,[a] eV	1.47	1.59	2.82	3.09	2.96	2.11
overlap population						
S–C (free SC_2H_4 = 0.560)	0.559	0.560	0.560	0.534	0.526	0.522
C–C (free SC_2H_4 = 0.737)	0.728	0.734	0.724	0.749	0.756	0.748
Mo1–S	0.585	0.584	0.510	0.361	0.463	0.417
Mo2, 3–S				0.461	0.398	0.377

[a] B.E. (binding energy) = E(Mo slab) + E(ethylene sulfide layer) − E(Mo + ethylene sulfide).

We model the surface by a slab of three layers of molybdenum atoms. This number has been shown to be a reasonable compromise between a convenient size of the calculation and an adequate representation of the surface.[15]

The choice of the unit cell was dictated by the necessity of keeping a relatively low coverage on the surface, otherwise the adsorbate molecules may come into close contact with one another, leading to high repulsive energies. With the chosen unit cell, the coverage will be 1/4 (one adsorbate molecule/four surface molybdenum atoms), and no short distances between adjacent adsorbate molecules are observed.

We took the Mo–S distance to be 2.44 Å, which is a very typical one, found in many molybdenum complexes.[3d,16] This constant distance implies that the height of the coordinating sulfur atom in the adsorbate above the surface will vary according to the multiplicity of the site. In what follows, we are going to consider three different adsorption sites: on top, **17a**; bridging between adjacent molybdenum atoms (nearest neighbors), **17b**; 3-fold, with the sulfur atom equidistant from Mo1, Mo2, and Mo4, **17c**. Having picked the adsorption sites, we have to decide on the

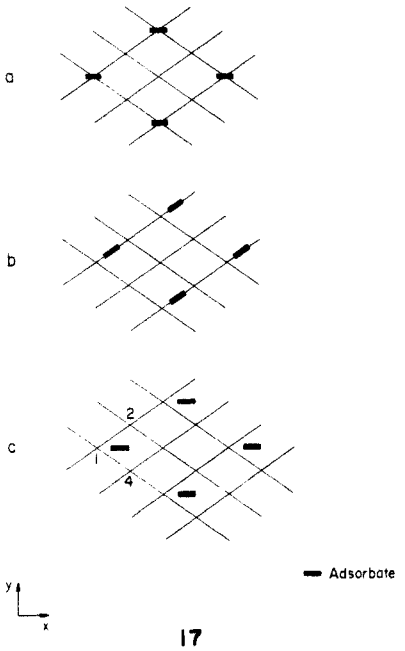

17

adsorption geometry. Both ethylene sulfide and trimethylene sulfide contain a planar SCC unit. From what we saw about their frontier orbitals, **2** and **3**, we may expect different interactions with one or more molybdenum atoms depending on the orientation of that ring. We shall consider, both for the top and 3-fold sites, limiting adsorbate geometries with the ring in the *xz* or *yz* plane; the corresponding situation for the 2-fold site will have the ring in the same plane as the Mo–Mo bond or perpendicular to it. These possible situations are sketched in **18**.

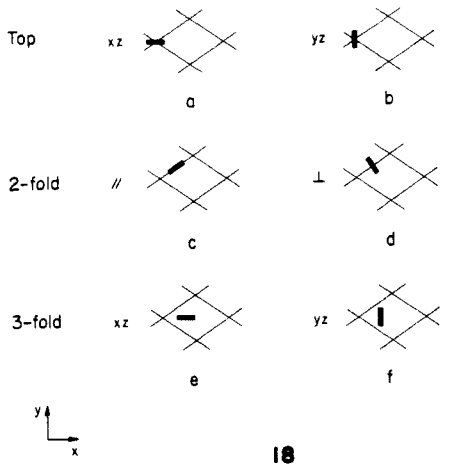

18

Allowing the ring to bend introduces other interesting possibilities, which will be discussed later.

Adsorption of Ethylene Sulfide

A first step in trying to understand how ethylene sulfide reacts on the molybdenum(110) surface involves finding its preferred adsorption site. In order to do that, we look at different parameters, such as, for instance, the binding energy of the adsorbate to the surface and the overlap population between the sulfur atom of the adsorbate and the molybdenum to which it binds. These and other important parameters are collected in Table I for several possible situations. A "bent" adsorbate means that the two carbons and their hydrogens move toward the surface, as measured by an angle, α, from the vertical, **19**.

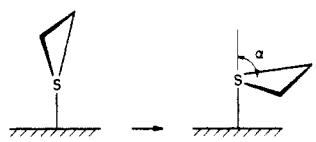

19

Let us start analyzing the results by looking at the binding energies. These are all positive, meaning that a stabilizing interaction has taken place between the adsorbate and the surface. Notice that the smaller values occur for on-top adsorption, where the adsorbate prefers to be bent. The opposite happens in the 3-fold site, where bending is decidedly unfavorable. This is the same trend that we observed for the bonding of ethylene sulfide to mono- and binuclear molybdenum complexes. The binding energies for the 2-fold and 3-fold sites are large and we cannot trust the difference between them, since they will depend on the exact Mo–S bond lengths, etc. We can conclude that all these sites are equally probable, more so than the top site. The bent 3-fold site is also probably excluded.

Strong molybdenum sulfur bonds are formed in all cases. Although the largest Mo–S overlap population is found for the top site, only one bond per unit cell is formed. For the 2-fold site,

(15) (a) Hoffmann, R. *Rev. Mod. Phys.* **1988**, *60*, 601. (b) Zheng, C.; Apeloig, Y.; Hoffmann, R. *J. Am. Chem. Soc.* **1988**, *110*, 749. (c) Zonnevylle, M. C.; Hoffmann, R. *Langmuir* **1987**, *3*, 452.

(16) (a) Carrondo, M. A. A. F. de C. T; Jeffrey, G. A. *Acta Crystallogr.* **1983**, *C39*, 42. (b) Section 36, Molybdenum. In *Comprehensive Coordination Chemistry*; Wilkinson, G., Ed.; Pergamon Press: Oxford, 1987; Vol. 3.

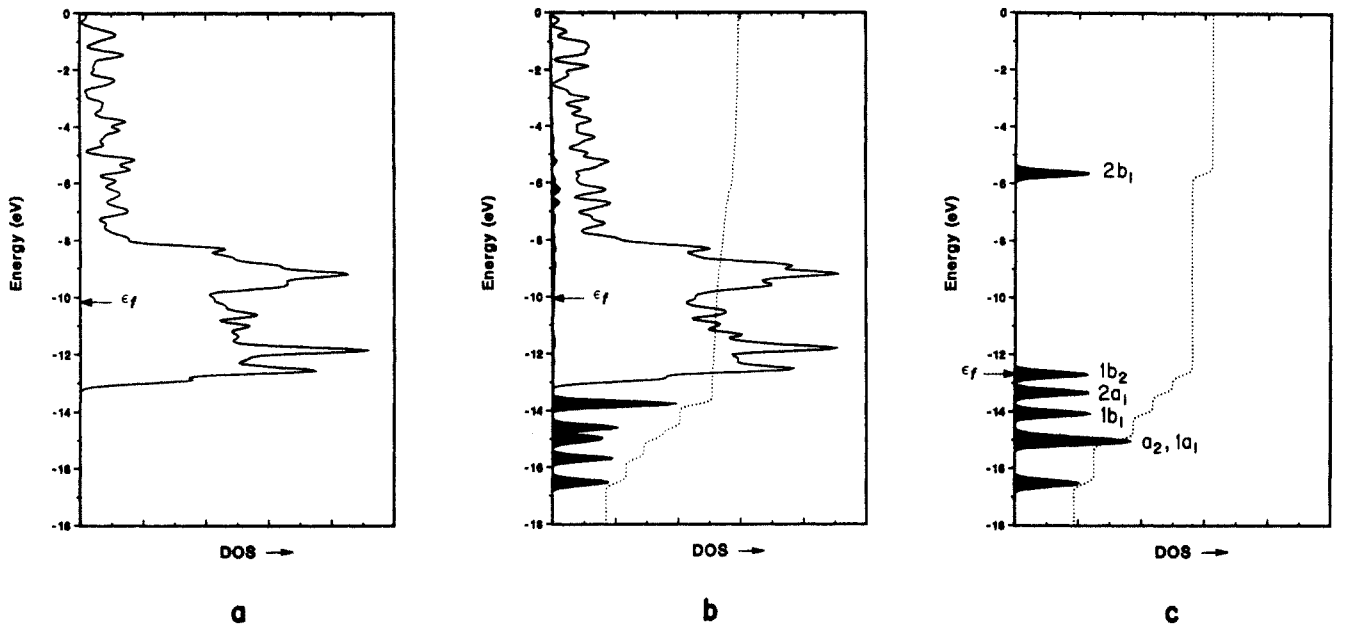

Figure 5. (a) Total density of states of the molybdenum slab before adsorption. (b) Total density of states (solid line) of ethylene sulfide adsorbed on Mo(110) on a 3-fold site (**18f**) and projection (dark area) and integration (dotted line) of the adsorbate states. (c) Total density of states (dark area) and integration (dotted line) of a layer of adsorbate before interaction with the surface (labels as in **2**).

Table II. Occupation of Ethylene Sulfide Orbitals after Adsorption on Mo(110)

	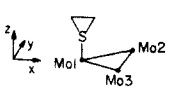					
$2b_1$ (LUMO)	0.040	0.034	0.077	0.059	0.052	0.063
$1b_2$ (HOMO)	1.882	1.815	1.594	1.538	1.552	1.616
$2a_1$	1.839	1.886	1.829	1.830	1.829	1.817
$1b_1$	1.968	1.969	1.944	1.806	1.744	1.785

two slightly weaker bonds are formed and three weaker ones are found for the different possibilities of 3-fold adsorption. Here, two different numbers are shown, as the bonds from S to Mo2 and Mo3 are different from the bond between Mo1 and S, even if the Mo–S distance is the same. While it is difficult to draw conclusions from these overlap populations, it seems that a stronger bond to the surface is formed in the 2-fold and 3-fold adsorption sites.

The remaining overlap populations in Table I give us some information about what happened to the ethylene sulfide molecule after adsorption. Changes in bond strengths due to the interaction with the surface may be indicative of the new reactivity the molecule exhibits. If we consider the free three-membered ring, the S–C overlap population is 0.560 and the C–C overlap population is 0.737. For both top and 2-fold sites, the S–C overlap population remains unchanged, while the C–C weakens. These sites are probably not precursors to gaseous ethylene formation. On the other hand, a simultaneous weakening of the S–C bond and strengthening of the C–C is observed when ethylene sulfide binds to the surface in the 3-fold site, suggesting an activation towards formation of ethylene, as is experimentally observed.

In order to understand these results, let us analyze the bonding of one of these sites in more detail. We can choose, for instance, the situation where the three-membered ring adsorbs in the 3-fold site, perpendicular to the surface, with its ring lying parallel to *yz*.

We show in the center of Figure 5 the total density of states (DOS) of a Mo(110) slab covered by an adsorbate layer. The dark area gives a projection of all the adsorbate states. These states were obtained by interaction of the Mo(110) slab states, shown on the left side of Figure 5, with those of the adsorbate layer, given on the right side. The molybdenum DOS is characteristic of its metallic properties, with no gaps. The s band penetrates the d band which lies between −8 and −13 eV. Sharp peaks are observed for the adsorbate layer DOS, as each molecule is quite far from its neighbors, thus resulting in very weak interactions. These sharp peaks can develop into broader bands by interaction with the Mo surface. Each peak is labeled according to the molecular orbital it is derived from in **2**.

Comparing the three parts of Figure 5, we can see more easily changes in the adsorbate DOS than in the molybdenum layer DOS. These indicate that some interaction is taking place. However, to understand which orbitals are involved in the bonding we must consider the projections of each of them individually.

This is shown in Figure 6 for several important ethylene sulfide orbitals. In (a) we see the projection of the three-membered ring HOMO, $1b_2$, solid line, with the respective integration (dotted line). There is still one main peak, but the integration shows this fragment orbital to be spread over a large energy range; ~15% of the states are localized in the Mo d region. In addition, the main peak is pushed down from ~12.5 to ~13.5 eV, due to interaction with the surface. $1b_2$ interacts especially effectively in the 3-fold site. Something similar is happening with the other two orbitals shown in Figure 6, parts b and c, which are respectively the other sulfur lone pair $2a_1$ and the molecular orbital $1b_1$. After adsorption, some of the ethylene sulfide states are partially vacated, their electrons transferred to molybdenum states. This transfer of electrons from the sulfur ligand to the metal can also be seen in the occupation of the levels mentioned, shown in Table II, which includes the other adsorption sites as well. We can see that the $1b_1$ level is only significantly depopulated in the 3-fold sites. $2a_1$ and $1b_2$ are depopulated for all of the sites, although $1b_2$ is more so for the higher coordination sites.

The bonding characteristics of the adsorbate levels are shown in the Crystal Orbital Overlap Population (COOP) curve of Figure 7. While the HOMO ($1b_2$) is essentially nonbonding and $2a_1$ is C–C bonding, $1b_1$ is simultaneously S–C bonding and C–C antibonding. If it is depopulated, the S–C bond will be weaker

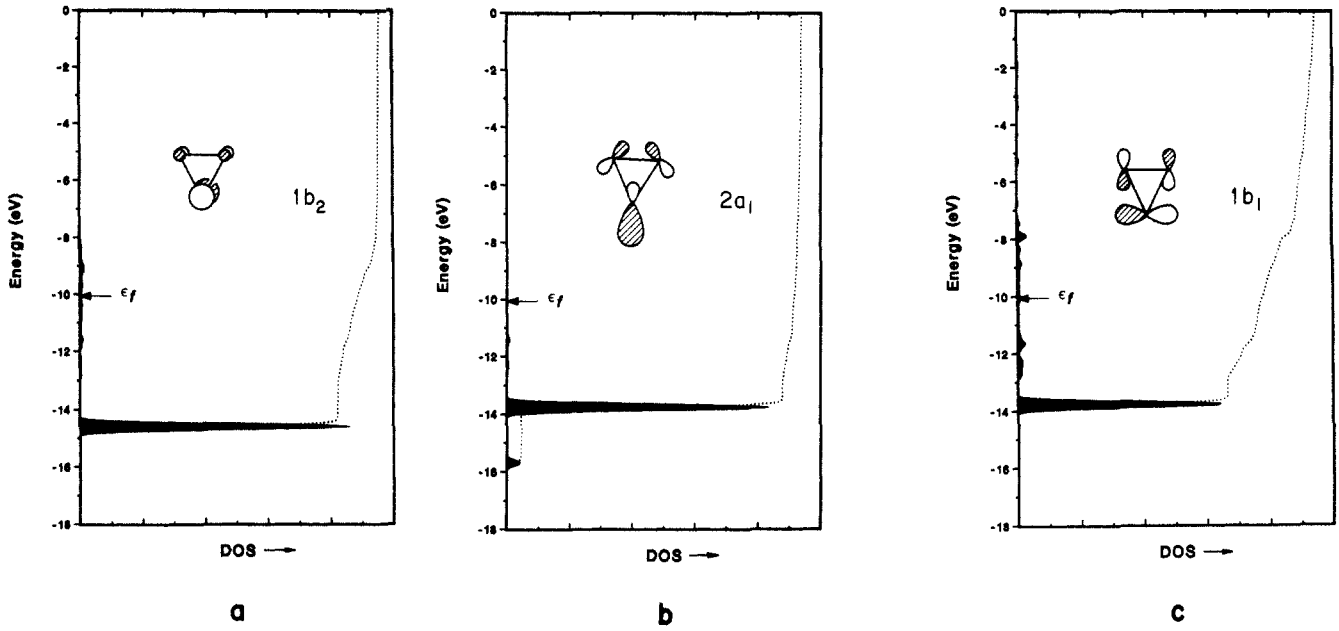

Figure 6. Projection (dark area) and integration (dotted line) of three ethylene sulfide orbitals after interaction with the Mo(110) surface: (a) the HOMO, $1b_2$; (b) $2a_1$; (c) $1b_1$.

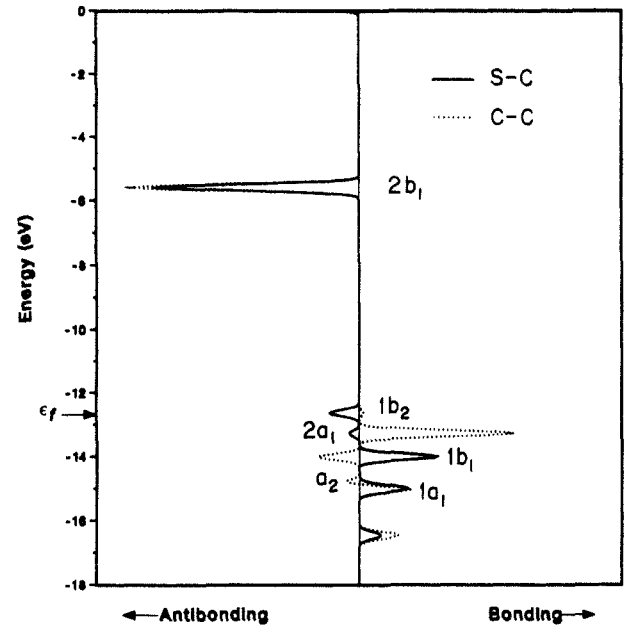

Figure 7. Crystal Orbital Overlap Population (COOP) curve depicting the bonding properties of the ethylene sulfide levels relative to the S–C and C–C bonds.

and the C–C bond stronger. That is a step toward breaking the S–C bonds and producing ethylene.

The ethylene sulfide LUMO ($2b_1$) interacts strongly with surface levels, as can be seen in Figure 5 (the peak of 5c is completely broken up). However, this level is only weakly populated, as the states it gives rise to are essentially above the Fermi level. This is important because the major cause of weakening of C–S and strengthening of C–C bonds upon adsorption is not population on this LUMO but depopulation of $1b_1$.

Adsorption of Trimethylene Sulfide

Trimethylene sulfide is not expected to behave very differently from ethylene sulfide as both its geometry (around the coordinating sulfur atom) and its frontier orbitals (**3**) are similar. Some results concerning adsorption in 2- and 3-fold adsorption sites are collected in Table III.

The binding energies are positive for both the 2-fold and 3-fold sites, but they become much smaller when the adsorbate is bent 50° down from perpendicular. Strong Mo–S bonds are formed

Table III. Binding Energies and Overlap Populations for Trimethylene Sulfide on Mo(110)

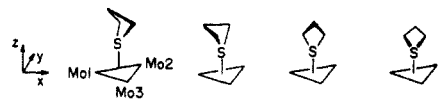

adsorption site, geometry	**18d**, perp.	**18f**, perp.	**18e**, perp.	**18e**, bent 50°
B.E., eV	2.66	2.30	2.75	1.75
overlap population				
S–C (free SC_3H_6 = 0.627)	0.628	0.603	0.608	0.597
C–C (free SC_3H_6 = 0.708)	0.705	0.693	0.707	0.708
C···C (free SC_3H_6 = −0.099)	−0.099	−0.089	−0.087	−0.086
Mo1–S	0.518	0.469	0.322	0.320
Mo2–S	0.518	0.366	0.457	0.353
Mo3–S		0.366	0.463	0.450

Table IV. Parameters Used in the Extended Hückel Calculations

atom	orbital	H_{ii}, eV	ζ_1	ζ_2	C_1[a]	C_2[a]
Mo	5s	−8.34	1.96			
	5p	−5.24	1.90			
	4d	−10.50	4.54	1.90	0.5899	0.5899
S	3s	−20.0	1.817			
	3p	−13.3	1.817			
C	2s	−21.4	1.625			
	2p	−11.4	1.625			
H	1s	−13.6	1.300			

[a] Coefficients used in the double-ζ expansion of the 4d orbitals.

(more nonequivalent Mo–S bonds are now formed, due to the nonplanarity of the adsorbate) in a comparable way to ethylene sulfide. The S–C bond is weakened by adsorption on the 3-fold site, but not on the 2-fold, as can be seen from the respective overlap populations. The C–C bonds are kept mostly unchanged, except for the 3-fold adsorption with the C–S–C plane parallel to *yz*. If cyclopropane is to be formed following adsorption the two α-carbons have to approach each other to form a bond. The overlap population between them, denoted as C···C, is always negative, although small. Adsorption does not seem to activate this molecule, as opposed to what we saw happening for ethylene sulfide.

In Figure 8 are shown both the adsorbate layer (right) and molybdenum slab DOS (left) before adsorption, and the total DOS

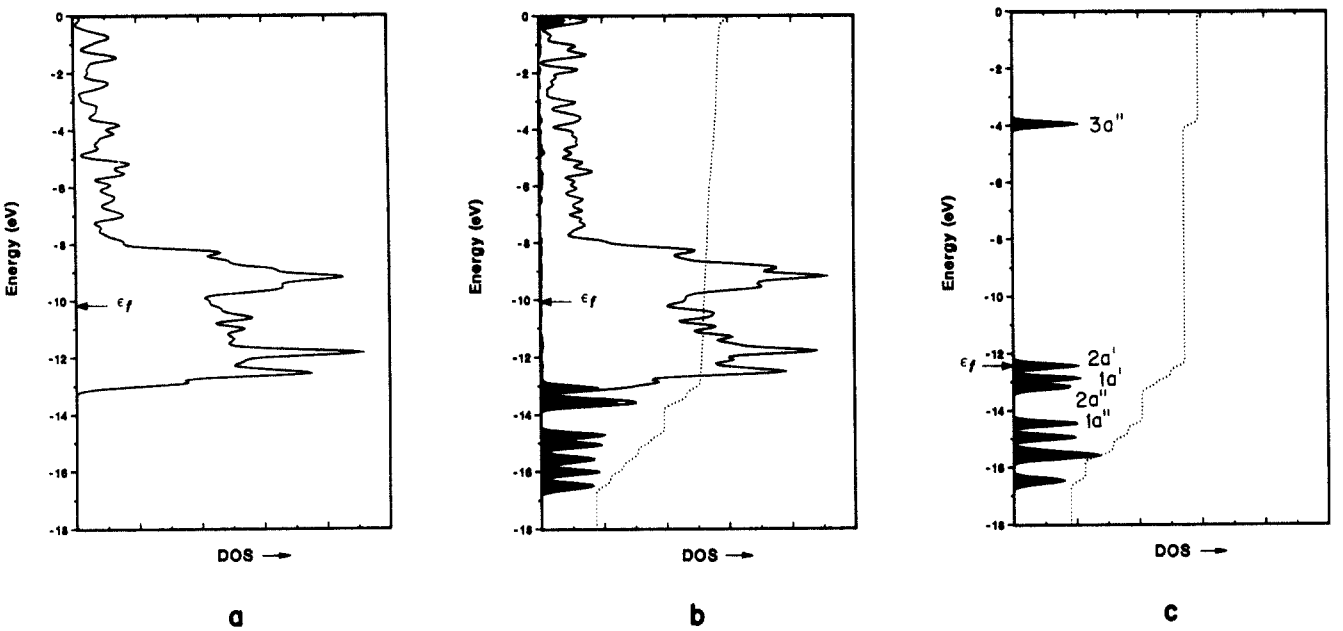

Figure 8. (a) Total density of states of the molybdenum slab before adsorption. (b) Total density of states (solid line) of trimethylene sulfide adsorbed on Mo(110) on a 3-fold site (**18f**) and projection (dark area) and integration (dotted line) of the adsorbate states. (c) Total density of states (dark area) and integration (dotted line) of a layer of adsorbate before interaction with the surface (labels as in **3**).

for the composite structure (center). Significant changes take place, indicative of the interaction between the two layers. A more detailed look at the adsorbate orbitals reveals that interaction proceeds mainly through the two highest occupied molecular orbitals, as they suffer the largest depopulation and the states spread across a considerable energy range. These are the two sulfur lone pairs; through them electrons are donated to the metal surface. On the other hand, the weaker interaction of the next two a″ levels (**3**) leads to weakening of the S–C bond, especially through the lower level, which has strong S–C bonding character. 2a″, which corresponds to the $1b_1$ orbital of ethylene sulfide, does not play a large role here, as participation of the sulfur atom in it is small, leading to a small contribution to the S–C overlap population. Although the band derived from the LUMO gets much wider, there is only a very small electronic transfer from the metal to the adsorbate. The net flow of electrons occurs in the opposite direction.

Reactions on the Surface

We saw in the preceding sections the extent to which ethylene sulfide and trimethylene sulfide were activated by interaction with the Mo(110) surface. In ethylene sulfide, activation toward formation of free ethylene and sulfided molybdenum was suggested by the overlap population changes, indicative of S–C bond weakening and C–C bond strengthening. However, nothing comparable was found for trimethylene sulfide. Although adsorption may induce S–C bond weakening, the two carbon atoms that are to form the new C–C bond are too far apart and there is only a very small and negative overlap population between them. This may indicate that the reaction of adsorbed ethylene sulfide will be easier.

We decided, however, to try and look for a potential energy surface for the two reactions, in order to be able to compare their characteristics. The same reaction as the one we used with the discrete molecular models was assumed. We chose for this study one of the preferred adsorption sites, namely the 3-fold one, with the SCC plane of the ring parallel to *yz* (**18f**), both for ethylene sulfide and trimethylene sulfide.

One must mention at this point the limitations of the extended Hückel method in dealing with reactions. From the beginning of the utilization of this approximate MO procedure it was clear that it does not predict distances well, even in molecules as simple as ethane, ethylene, and acetylene.[7a] So the method is not always reliable for comparing the energetics of two geometries differing substantially in bond length. Reaction profiles may be distorted.

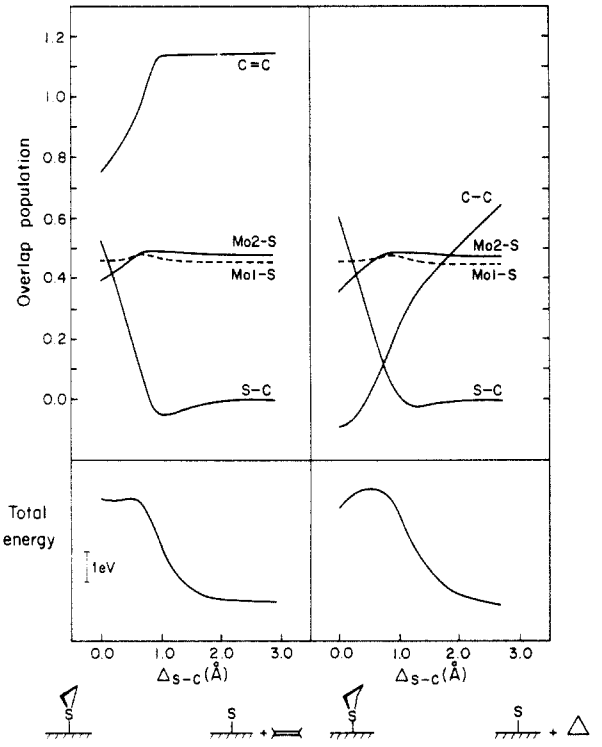

Figure 9. Variation of the S–C, C–C, and Mo–S overlap populations and total energy along the reaction path (see text) for producing ethylene from adsorbed ethylene sulfide (left) and cyclopropane from adsorbed trimethylene sulfide (right).

For a balanced assessment of the reliability of the method, see Lowe.[17] The method is nevertheless simple and transparent and catches most of the factors that determine bonding. With these reservations in mind, we use it here.

Figure 9 gives the change in total energy along the reaction and the variation in S–C, C–C, and Mo–S overlap populations for the reactions of both ethylene sulfide and trimethylene sulfide. The first thing to notice is how similar to **16** and Figures 2, 3,

(17) Lowe, J. *Quantum Chemistry*; Academic Press: New York, 1978; Chapter 10.

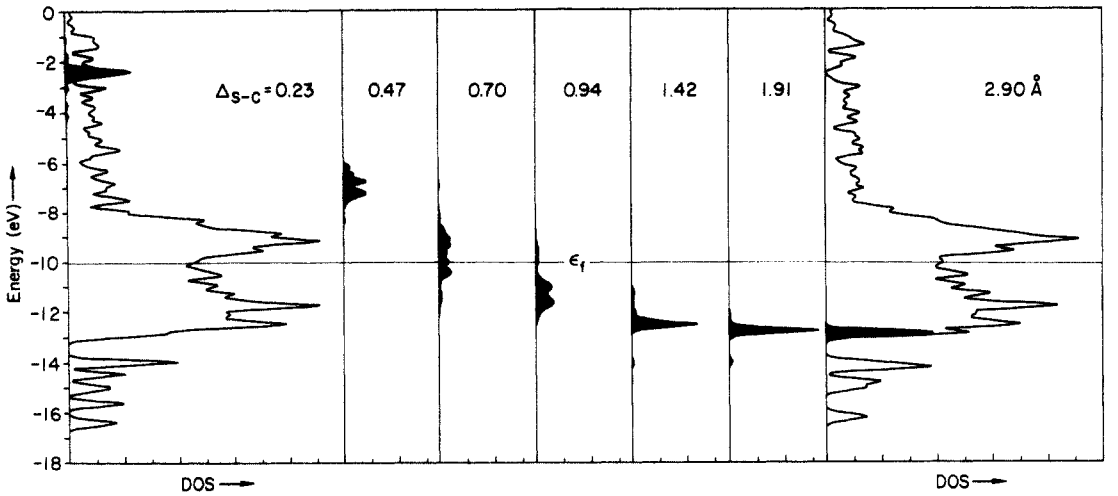

Figure 10. Projection of the a_1 molecular orbital of ethylene sulfide that becomes ethylene π after reaction on the Mo(110) surface, at different stages of the reaction measured by the stretching of the S–C bond. The total densities of states (surface and adsorbate) are shown at the two extremes considered.

and 4 these curves are, suggesting analogous evolutions of the different levels, even if there are so many more for a surface. As we saw before, in the Walsh diagram of Figure 2, the level that will end as ethylene π is greatly stabilized and drops below the d-block levels just after the transition state. We can detect this happening by the increase of the C–C overlap populations after this level becomes filled.

The same happens for the reaction on the surface (Figure 9a). We can then imagine that an orbital that will be ethylene π is going to drop below the Fermi level at some state of the reaction. It is then occupied, and the C–C overlap population increases, to become a characteristic one for a C–C double bond. Unfortunately, we do not have any easy way of constructing something analogous to a Walsh diagram for the reaction on the surface.

We tried, however, to look at one of the orbitals of the adsorbate that appears to play a crucial role in the reaction: the a_1 level that crosses other metal d a_1 orbitals and finally becomes the bonding π level of ethylene (Figures 2 and 3). We see a projection of that MO at various stages of the reaction (given by the stretching of the S–C bond, as previously, in Figure 10; note that it is not a linear scale), but we omitted the initial state. The chosen MO is outside the energy window, due to its strongly S–C and C–H antibonding character. Stretching the S–C bond and moving the hydrogens toward the nodal plane of the C p orbital (see **12**) makes it more and more stable as the reaction proceeds. Let us imagine that we consider the median of each projected peak and plot that energy as a function of the S–C bond stretching. The resulting curve is similar to what would happen in the Walsh diagrams of Figures 2 and 3 in the absence of level crossings. In the beginning of the reaction, the energy of this orbital is too high for it to interact much with the surface. As the reaction occurs, we observe a spread in energy, indicative of a stronger interaction. In the end that dispersion disappears, as the MO becomes π and the ethylene molecule is very far away from the surface.

Let us now compare the two reactions. The decomposition of ethylene sulfide occurs almost without any activation energy (less than 0.1 eV). On the other hand, there is an energy barrier, although small (0.4 eV), for the conversion of trimethylene sulfide to cyclopropane. This agrees extremely well with the estimated barriers, based on experimental results of <6 and 13 kcal/mol, respectively.[3a] If we take into account the changes in C–C bond length that occur during the reaction, we expect a decrease in the energy barrier for production of ethylene from ethylene sulfide accompanying the stabilization, due to the contraction of that bond. For production of cyclopropane from trimethylene sulfide, however, the change in C–C bond length is almost negligible, as pointed out before, so there should be no significant modification of the calculated barrier.

Concerning the evolution of the bonds, we see that as the S–C bond is broken, the C–C bond is strengthened or formed. Also, and this is slightly different for the surface, two of the Mo–S bonds become stronger when the S–C bonds break. This effect may be an important one in contributing to lowering the activation energy for the reaction.

Experimental results show that the evolution of ethylene is slowed down as the reaction proceeds and the molybdenum surface is getting more and more sulfided. In order to test this, we repeated the calculations for the reaction, adding to the surface sulfur atoms in a 1/4 coverage. The sulfur atoms were made to occupy 3-fold sites, as that is their usual preference. Both energy and overlap population change as they did in the absence of added sulfur. If these results are to be trusted, it means that the slowing down of the reaction is due not to the electronic influence of co-adsorbed sulfur but to the lack of suitable sites for the ethylene sulfide molecules to adsorb and react.

Let us now turn to the possibility of other, non-concerted reactions occurring on the adsorbed cyclic sulfides. In these one imagines only one of the S–C bonds is broken at first, instead of two. Such an asymmetry may be induced by hydrogen. The presence of hydrogen does not change the kinetics of the concerted reaction. However, one of the alternative paths, B in **1**, requires hydrogen in order that a terminal methyl group be formed. We wanted to see if hydrogen coadsorption also influences path A. We note, however, that experimentally[3c] coadsorption of atomic hydrogen on trimethylene sulfide does *not* alter the kinetic formation or the yield of cyclopropane, suggesting that hydrogen-assisted C–S bond activation is not occurring. In contrast the presence of surface hydrogen increases the kinetics and yield of propane formed via the thiolate intermediate, suggesting the possibility of hydrogen-assisted C–S bond weakening in pathway B. We introduced the one hydrogen atom per unit cell (coverage 1/4) in the two following situations: adsorbate in 3-fold site, perpendicular, with C–S–C plane parallel to *xz* and hydrogen in another 3-fold site, **20**; adsorbate in 3-fold site but bent 50° toward *y* from its position, with hydrogen on top of Mo2, **21**.

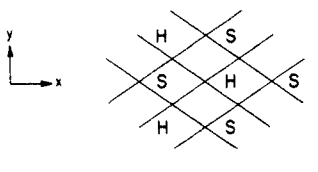

20

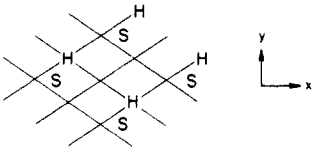

21

In **20**, the hydrogen coadsorbate is quite removed from the trimethylene sulfide molecules. There are no steric repulsions. But on the other hand, there is no activation either. The intramolecular and Mo–S overlap populations do not change when hydrogen is coadsorbed. The situation changes, however, for **21**. Now the hydrogen is very close to one of the CH_2 groups and this arrangement is energetically unfavorable. The asymmetry introduced by the hydrogen produces one slightly weaker S–C bond, with overlap population 0.611, and a stronger one (overlap population 0.637), compared to the free adsorbate. Also, a strong bond between the hydrogen and the carbon of the nearest methylene group develops (overlap population 0.332). This is not surprising given the short C–H distance, 1.189 Å. We can tentatively assume from this that if there is hydrogen on the surface and if it approaches the adsorbate in the proper manner the formation of a C–H bond induces breaking of preferentially one S–C bond.

Another way of obtaining the same result is by considering a tilting movement of the adsorbed sulfide, as sketched in **22**, where the ring on the right is tilted by β.

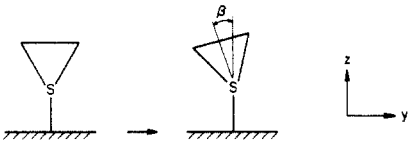

22

When we do this, the energy increases quite slowly with β, especially for ethylene sulfide. One of the S–C bonds weakens with the simultaneous strengthening of the other one. This was calculated for the sulfur ligand in a 3-fold site, the ring plane lying parallel to xz (**18e**). As the ring is tilted, a carbon atom approaches one of the Mo atoms, **23**.

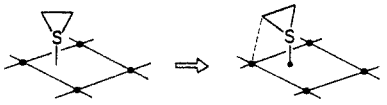

23

This approach may facilitate transfer of a hydrogen to carbon with breaking of the S–C bond and formation of a thiolate intermediate.

From this, the process seems more likely for the three-membered ring, where we know tht it does not take place. A possible explanation is that the competing reaction to form ethylene by a concerted process occurs more easily (there was no barrier for it). However, for trimethylene sulfide, there is some barrier to form cyclopropane concertedly. A competing mechanism then has a better chance.

Discussion

Our calculations suggest that cyclic sulfides prefer to adsorb on 2- or 3-fold sites, a distinction between these being impossible to make on the basis of our results. Similar bonding preferences are expected for longer alkyl chain sulfides, as the nature of the frontier orbitals of the adsorbates will not be greatly changed. The bonding takes place essentially by donation of electrons from sulfur lone pairs to molybdenum empty levels. Only in ethylene sulfide is there a significant contribution to the bonding from a S–C bonding, C–C antibonding orbital, which we think is responsible for activating the molecule toward ethylene formation. We found that back donation from the Mo(110) surface to the LUMO of the cyclic sulfides plays only a minor role in the bonding.

The interaction of cyclic sulfides with a different surface, Cu(110),[18] was studied by means of ultraviolet photoelectron spectroscopy, and it differs markedly from that of Mo(110), in that only ethylene sulfide reacts to give off ethylene (which was not detected) and surface sulfur, while the other sulfides just adsorb. The authors describe the bonding qualitatively as being mainly electron donation from the sulfur lone pair to empty 4s, 4p orbitals on copper, accompanied by back-donation from copper to adsorbate states that fell below the Fermi level. They do not try to make a correlation with the reactivity.

The ethylene sulfide ring, eventually containing substituents, is very easily desulfurized by reagents such as RLi and $Fe_2(CO)_9$, $Fe_3(CO)_{12}$,[19a] or $RP{=}W(CO)_5$,[19b] for instance, where the ethylene that is formed reacts with the phosphorus atom. This reactivity agrees with the results we obtained for the molybdenum molecular models, although we must keep in mind the existing differences.

A reaction that comes closer to the one on the surface involves cyclic sulfides and molybdenum vapor.[20] Ethylene sulfide is cleaved, with evolution of gaseous ethylene and formation of a molybdenum sulfide species. However, as opposed to the reaction on Mo(110), trimethylene sulfide gives only cyclopropane and propene. The mechanism of the reaction is far from well understood, but apparently a biradical intermediate is not involved.

Another interesting aspect is the suggestion of the formation of a pentacoordinate sulfur intermediate preceding olefin formation when ethylene sulfides react with RLi.[18] This is comparable to the coordination of sulfur on the 3-fold site that we tentatively propose to be one of the most activating.

Much work has been done in order to understand how reactions occur on surfaces and why several crystal faces exhibit different adsorption and reactivity patterns, an example being the reduction of nitric oxide, NO, on platinum.[21] A few models have been proposed, which deal with the characteristics of the adsorbate–surface interaction in the initial stages of the reaction. On the other hand, it was suggested, although in the context of another type of catalytic reactions, that the interaction with the transition state, not with the initial state, is determinant of the catalyst activity.[22] This idea was not very straightforward to apply to the comparison of the reactions of ethylene and cyclopropane formation from C_2H_4S and C_3H_6S, respectively, on Mo(110). One of the difficulties, and this is different from other studied reactions,[15b,21] is that the gaseous ethylene products formed are not trapped by the surface.[3b,c,f] The surface only acts on the reaction through the sulfur atom of the cyclic sulfide. This was the reason that led us to follow a specific pathway for the two reactions, even with all the limitations involved. As the ring size increases, more severe geometric changes are needed for a concerted reaction, increasing the activation energy, thus making that reaction path less and less competitive, with, for instance, selective breaking of only one S–C bond. We saw earlier how this could be induced either by coadsorbed hydrogen or by tilting movements of the adsorbate which do not require too much energy. A more detailed study of this alternative mechanism is, unfortunately, outside our calculational possibilities, due to the enormous number of degrees of freedom involved.

Acknowledgment. M.J.C. is grateful for a NATO Fellowship, which supported her stay at Cornell. M.J.C. also thanks Marja Zonnevylle for helpful discussions and suggestions. Our work was supported by the National Science Foundation, Grant DMR 85-16616-AO2. We thank Jane Jorgensen and Elisabeth Fields for the drawings and Joyce Barrows for the production of this manuscript.

Appendix

All the calculations were of the extended Hückel type,[7] with the tight-binding approach[8] for the surface calculations. The

(18) Thomas, T. M.; Grimm, F. A.; Carlson, T. A.; Agron, P. A. *J. Electron Spectrosc. Rel. Phenom.* **1982**, *25*, 159.

(19) (a) Trost, B. M.; Zimon, S. D. *J. Org. Chem.* **1973**, *38*, 932. (b) Marinetti, A.; Mathey, F. *Organometallics* **1987**, *6*, 2189.

(20) Reid, A. H.; Shevlin, P. B.; Webb, T. R.; Yun, S. S. *J. Org. Chem.* **1984**, *49*, 4728.

(21) (a) Banholzer, W. F.; Park, Y. O.; Mak, K. M.; Masel, R. I. *Surf. Sci.* **1983**, *128*, 176. (b) Masel, R. I. *Catal. Rev.-Sci. Eng.* **1986**, *28*, 335.

(22) Wolfenden, R.; Frick, L. *J. Protein Chem.* **1986**, *5*, 147.

parameters used are collected in Table IV.

The distances taken in the molecular models $MoH_4(SC_nH_m)^{4-}$ and $Mo_2H_6(SC_2H_4)^{6-}$ were respectively Mo–H = 1.80 Å, Mo–S = 2.44 Å, Mo–Mo = 2.72 Å. Ethylene sulfide and trimethylene sulfide were considered to have the same geometry as determined for the free molecules. The two-dimensional molybdenum surface consisted of three layers. The adsorbate coverage was kept at $^1/_4$ throughout all the calculations.

Sets of 6K or 8K points in the irreducible wedge of the oblique unit cell in reciprocal space were used, according to the symmetry of the problem. They were chosen following the geometrical method of Ramirez and Böhm.[23]

Registry No. SC_2H_4, 420-12-2; SC_3H_6, 287-27-4; Mo, 7439-98-7.

(23) Ramirez, R.; Böhm, M. C. *Int. J. Quantum Chem.* **1986**, *30*, 391.

Resonance Interactions in Acyclic Systems. 1. Energies and Charge Distributions in Allyl Anions and Related Compounds

Kenneth B. Wiberg,* Curtis M. Breneman, and Teresa J. LePage

Contribution from the Department of Chemistry, Yale University, New Haven, Connecticut 06511. *Received December 27, 1988*

Abstract: The energies of dissociation of propane to 1-propyl cation and anion and of propene to allyl cation and anion may be satisfactorily reproduced via ab initio calculations at the MP4/6-311++G**//6-31G* level. The reaction of 1-propyl cation with propene to give the unconjugated allyl cation was found to be endothermic, whereas the corresponding reaction of the anion was exothermic. The rotational barrier for allyl cation was 36 kcal/mol, whereas that for the anion was 19 kcal/mol. These data were analyzed in terms of electron delocalization and the electrostatic energies of the ions, and it was concluded that whereas the cation had significant resonance stabilization, the anion had little stabilization. A series of allyl type anions were examined making use of 6-311++G** wave functions calculated at the 6-31G* geometries. Correction for electron correlation at the MP3 level led to calculated proton affinities which agreed well with the experimental values. Electronegative atoms at the central position had little affect on the proton affinities, but when they were at the terminal positions, there was a large change. The changes in electron population among the anions were studied via numerical integration of the charge densities within boundaries which may be assigned to the atoms in the ions. The more stable anions are characterized by a $-+-$ charge distribution for the three atoms in the allylic system, leading to internal coulombic stabilization.

Allyl Anion and Cation

Allyl anion systems such as A=B—C^-↔$^-$A—B=C are commonly observed, and generally are considered to be stabilized by electron delocalization.[1] However, recent discussions of the origin of the acidity of carboxylic acids[2,3] and other acids such as nitrous acid[4,5] have suggested that the resonance stabilization of the anions may not be the more important factor in leading to increased acidity. In view of the importance of these species, we have carried out a study of the energies and charge distributions of a number of types of allyl anions.

We shall first examine allyl cation and anion and compare their energies with those for 1-propyl cation and anion, respectively. The cations and anions have received considerable experimental[6,7] and theoretical[8,9] study, but there are important aspects of these systems which have not as yet been explored. The 6-31G* optimized geometries for many of the compounds are available,[10] and we calculated the structures for 1-propyl and allyl anions. The energies were calculated by using the 6-311++G** basis set[11] which is effectively triple-ζ and includes both diffuse functions and polarization functions at all atoms. This was chosen to allow adequate flexibility in describing the charge density distribution. A triple-ζ basis allows the "size" of each atom to be well represented, the diffuse functions allow a better description of lone pairs and anionic sites,[12] and the polarization functions improve the description of the charge density in the region between atoms having different electronegativities. The calculated energies are given in Table I. In addition, the energies of the allyl ions which had been rotated by 90° about one of the C–C bonds to give π-unconjugated ions were obtained and are included in Table I.

The calculated ionization energies of propane and of propene are compared with the experimental data[13] in Table II. The former must be corrected for the charge in zero-point energy caused by breaking one C–H bond. This will involve one C–H stretching vibration and two C–H bending vibrations. The vi-

(1) Wheland, G. W. *Resonance in Organic Chemistry*; Wiley: NY, 1955.
(2) Siggel, M. R.; Thomas, T. D. *J. Am. Chem. Soc.* **1986**, *108*, 4360. Siggel, M. R.; Streitwieser, A., Jr.; Thomas, T. D. *Ibid.* **1988**, *110*, 8022.
(3) Wiberg, K. B.; Laidig, K. E. *J. Am. Chem. Soc.* **1987**, *109*, 5935.
(4) Wiberg, K. B. *Inorg. Chem.* **1988**, *27*, 3694.
(5) Thomas, T. D. *Inorg. Chem.* **1988**, *27*, 1695.
(6) Allyl cations: Olah, G. A.; Comisarow, M. B. *J. Am. Chem. Soc.* **1964**, *86*, 5682. Schleyer, P. v. R.; Su, T. M.; Saunders, M.; Rosenfeld, J. C. *J. Am. Chem. Soc.* **1969**, *91*, 5174. Deno, N. C.; Haaddon, R. C.; Novak, E. N. *J. Am. Chem. Soc.* **1970**, *92*, 6991.
(7) Allyl anions: (a) Thompson, T. B.; Ford, W. T. *J. Am. Chem. Soc.* **1979**, *101*, 5459. (b) Brownstein, S.; Bywater, S.; Worsfold, D. *J. Organomet. Chem.* **1980**, *199*, 1.
(8) Allyl cations: (a) Mayr, H.; Forner, W.; Schleyer, P. v. R. *J. Am. Chem. Soc.* **1979**, *101*, 6032. (b) Raghavachari, K.; Whiteside, R. A.; Pople, J. A.; Schleyer, P. v. R. *Ibid.* **1981**, *103*, 5649. (c) Cournoyer, M. E.; Jorgensen, W. L. *Ibid.* **1984**, *106*, 5104.
(9) Allyl anions: Clark, T.; Rohde, C.; Schleyer, P. v. R. *Organometallics* **1983**, *2*, 1344.
(10) *Carnegie-Mellon Quantum Chemistry Archive*; 3rd. ed.; Whiteside, R. A.; Frisch, M. J.; Pople, J. A., Eds.; Carnegie-Mellon University: Pittsburgh, PA, 1983; ref 8.
(11) Basis sets: 6-31G*, Hariharan, P. C.; Pople, J. A. *Chem. Phys. Lett.* **1972**, *16*, 217. 6-311G*, Raghavachari, K.; Binkley, J. S.; Seeger, R.; Pople, J. A. *J. Chem. Phys.* **1980**, *72*, 650; 6-31+G*, Clark, T.; Chandrasekhar, J.; Spitznagel, G. W.; Schleyer, P. v. R. *J. Comput. Chem.* **1983**, *4*, 294.
(12) Chandrasekhar, J.; Andrade, J. G.; Schleyer, P. v. R. *J. Am. Chem. Soc.* **1981**, *103*, 5609.
(13) Lias, S. G.; Bartmess, J. E.; Liebman, J. E.; Holmes, J. L.; Levin, R. D.; Mallard, W. G. *Gas Phase Ion and Neutral Thermochemistry*, American Institute of Physics: 1988.

0002-7863/90/1512-61$02.50/0